# INDUCING HYDROPHOBICITY IN CELLULOSE BY USING POLYVINYLIDENE DIFLUORIDE (PVDF) TO PRODUCE FREE-STANDING CELLULOSE/PVDF COMPOSITE FILMS

RAJKUMAR DEY,[*] SHAMIMA HUSSAIN[**] and ARUN KUMAR PAL[*]

[*]*Department of Instrumentation Science, Jadavpur University, Kolkata 700032, India*
[**]*UGC-DAE CSR, Kalpakkam Node, Kokilamedu 603104, India*
✉ *Corresponding author: A. Kumar Pal, msakp2002@yahoo.co.in*

*Received* September 12, 2019

The sol-gel technique was utilized to prepare cellulose free-standing films using polyvinylidene flouride (PVDF) to induce hydrophobicity to inherently hydrophilic cellulose. The films were characterized by FTIR, Raman, SEM and XRD measurements. Contact angles of the water droplets placed on the prepared films were measured to ascertain their degree of hydrophobicity. The contact angle increased from 10° to 147° with the increase in the PVDF content, and then decreased with further addition of PVDF. The highest contact angle (147°) was obtained for the cellulose/PVDF composite films with 42 wt% PVDF. The results were interpreted in terms of the interaction of the bonding of hydrogen molecules in water, modulating the nature of the surface of the cellulose/PVDF composite films.

***Keywords***: cellulose, hydrophobicity, Raman, FTIR

## INTRODUCTION

Recently, imparting hydrophobicity to inherently hydrophilic cellulose has gained the attention of the scientific community. Cellulose films and papers have become technologically important due to their wide variety of functional applications, including water-repellent outdoor clothing, bandages, and hydrophobic papers.[1] Cellulose paper has excellent mechanical properties, such as flexibility and foldability.[2] It is also a low-cost, recyclable, mechanically stable and environmentally friendly material.[3] Cellulose paper has also attracted interest as a substrate for photovoltaic cells due to its various advantageous properties. Besides being inexpensive and eco-friendly, some obvious advantages are its good flexibility, biodegradability, light weight and foldable character, which are required for portable electronics. However, cellulose paper made out of cellulose fibers with inherent hydrophilic character would not be conducive to the industrial developments in the above-mentioned area of scientific interest. Moreover, cellulose cast on various materials sticks strongly to the surface due to strong –OH bonding associated with cellulose. This makes the production of free-standing cellulose films not conducive to industrial application. Thus, one has to overcome the above two problems before rendering cellulose paper suitable for electronic applications, utilizing multilayer structures.

A growing demand for "greener" products has been remarked and scientists are engaged in exploring natural raw materials, including plant triglycerides and oils to impart hydrophobicity to cellulose.[4-6] Huang *et al*.[6] tried to reduce the hydrophilic character of cellulose fibers utilizing chemical surface modification with hydrophobic compounds. Due to the above advancement, research on cellulose fibers in the field of bio-applications has attracted renewed interest and the subject has been on the anvil. Nevertheless, there is still a pressing demand to investigate the formation of water-repellent cellulose fibers *via* more environment friendly and renewable resources, as apparent from current reports on this issue.

Awa *et al.*[7] investigated the effects of crystallinity in microcrystalline cellulose on the hydrophilic properties of tablets. It was observed that water penetration and moisture absorbability

of the tablets increased with a decrease in crystallinity. Yu *et al.*[8] prepared micro/nano texturized oxidized cellulose membranes by constructing a layer-by-layer assembly with a base cellulose film. The surface was modified by covalent linkages with amino-functionalized silica nanoparticles (260 nm diameter) and epoxy-functionalized silica nanoparticles (30 nm diameter). They observed that a five-layered nanoparticle cellulose membrane became super-hydrophobic, having a water contact angle of 151° ± 2°. He *et al.*[9] reported the formation of highly hydrophobic cellulose composite films. These films were obtained *via* solvent-vaporized controllable crystallization of stearic acid in the porous structure of cellulose films. They concluded that the crystallization of stearic acid induced by the pore wall of the cellulose matrix was responsible for forming a micronano binary structure. This resulted in a rough surface formed by micro/nano spaces on the films. These micro/nano spaces on the film surface trapped air abundantly, leading to the observed hydrophobicity. Adewuyi *et al.*[10] modified the surface of cellulose with the introduction of an ester functional group *via* a simple reaction method. They observed a significant improvement in hydrophobicity after the above modification. Wang *et al.*[11] studied the dissolution of cellulose in aqueous solutions. It was observed that greater hydrophobicity in cellulose culminated in stronger dissolution power.

An improvement in the properties of cellulosic textile fibers was reported by Huang *et al.*[12] by using betulin. Substantially improved hydrophobicity, with a water contact angle of 136°, was achieved in their work. Studies on super-water-repellent oil sorbents based on cellulose acetate mats were presented by Mikaeili and Gouma.[13] They reported a single-step synthesis route for the above synthesis. The spun fibers presented a water contact angle of 154.3°. Yuan *et al.*[14] observed an enhancement in the hydrophobicity of nano-fibrillated cellulose through grafting of alkyl ketene dimer. Recently, Lim *et al.*[15] reported that the liquid resistance/repellency is dependent on solid surface energy and roughness, and surface modifications. They provided a geometric model of a nanoscale surface, which led to designing cellulose acetate (CA) nanofibers by entrapping $SiO_2$ nanoparticles.

Printable and flexible electronics have gained considerable attention over the past 10 years due to their broad application in devices with a substantial societal impact. They include flat displays, optoelectronics, radio-frequency identification tags, sensors and flexible electronic devices for the community.[16–19] Polyvinylidene fluoride (PVDF) is extensively used as an ultrafiltration membrane material in a wide range of applications due to its outstanding mechanical strength, chemical resistance and thermal stability.[20] In this work, the results of our investigation on the possibility of initiating hydrophobicity in inherently hydrophilic cellulose by adding an appropriate amount of PVDF to produce cellulose/PVDF free-standing and flexible films are reported. We have used the sol-gel route for the above synthesis. FESEM, FTIR, Raman and XRD measurements were used to characterize the developed films. The contact angles of water droplets placed on the achieved free-standing cellulose/PVDF films were measured to ascertain their hydrophobic nature.

## EXPERIMENTAL

### Materials and analytical equipment

For this study, cellulose fibers of an average size of ~100 μm were obtained from Sigma-Aldrich Co.

A Carl Zeiss AURIGA FESEM was used to record the surface morphology at an operating voltage of 5 kV in the secondary emission mode. A Renishaw inVia micro-Raman spectrometer (514 nm Argon laser) was used for Raman studies. Micro-structural information was obtained from X-ray diffraction (XRD) measurements, carried out using a Rigaku MiniFlex XRD (0.154 nm CuKα line). FTIR spectra were recorded in the range of 400-4000 $cm^{-1}$ by using a NicoletTM-380 FTIR. Water contact angle measurements were performed in the static mode, using appropriate laboratory instrumentation. A droplet of deionized water (~5 μL) was placed on the film surface, using a microsyringe. All reported contact angle data were obtained by averaging 3 points on each surface. The values were recorded after the contact angle equilibrated.

### Synthesis of free-standing and flexible cellulose paper

For the synthesis of free-standing and flexible cellulose paper, a fixed amount of cellulose fibers (800 mg) was placed in several conical flasks. PVDF powder was then added in different proportions to the above conical flasks containing cellulose. A fixed amount of dimethylformamide (DMF ~7 mL) was then added to the above mixtures. All the mixtures were refluxed for 1 h, with constant stirring, at room temperature for complete dissolution of the solute. The final solution was obtained after 4-5 h refluxing, with constant stirring at 60 °C. Initiation of gelation was

then observed. The above solution was used to cast cellulose/PVDF free-standing and flexible films. The films were uniformly applied as coating on a glass substrate at room temperature, using a two-stage spin coater at a low spin (60 rpm) and subsequently at 200 rpm. The films were annealed by using a microwave oven, which was operated at 100 W power level for 3 min. The films could be easily peeled from the glass substrate. The flexible free-standing films thus obtained were used for characterization. The thickness of the composite films was ~100 µm and the active film area was ~10 mm x 10 mm.

## RESULTS AND DISCUSSION

### Hydrophobicity in cellulose/PVDF free-standing films

We have measured the contact angle of water droplets placed on the developed films, as discussed in the section above. Photographs of the water droplets placed on the pure cellulose and pristine PVDF films are shown in Figure 1a and 1b, respectively. It may be observed that the water droplet was absorbed almost instantly by the pristine cellulose film because of its basic hydrophilic nature (Fig. 1a). The pristine PVDF film indicated a contact angle of ~98$^o$ (Fig. 1b and inset of Fig. 1a).

It was interesting to study the modulation of the basic hydrophilic characteristic of cellulose with the addition of PVDF initiating hydrophobic characteristics in these cellulose/PVDF composite films. The hydrophobicity of the above free-standing films with increased PVDF content was studied. Photographs of water droplets placed on these films are shown in Figure 1 (c-i).

With increased addition of PVDF to cellulose to form cellulose/PVDF free-standing paper (as described in the previous experimental section), the shape of the water droplets changed from hemispherical to nearly spherical and then back to hemispherical ones (Fig. 1c-i). The variation of the contact angle with the PVDF content in cellulose, as determined from the above figures, is shown in the inset of Figure 1a. It is apparent from it that the contact angle increased from 10$^o$ for the pristine cellulose film to 147$^o$ for the films containing 42 wt% of PVDF. With further addition of PVDF to the cellulose, a decrease in the contact angle was observed.

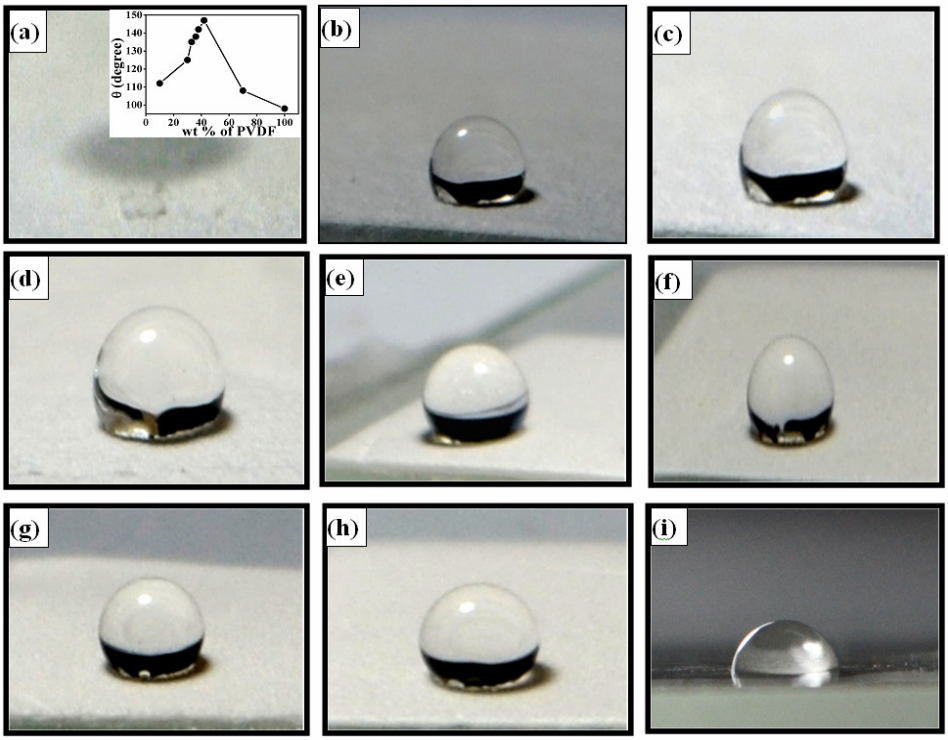


Figure 1: Photographs showing hydrophobicity in (a) cellulose (inset shows the variation of contact angle with PVDF concentration in cellulose/PVDF films, (b) PVDF, and (c)-(i) cellulose/PVDF films with increasing PVDF concentration (10, 30, 33, 36, 38, 42, 70 wt%)

It is apparent that the highest contact angle (~147$^o$) was obtained with the addition of 42 wt% PVDF to cellulose. Thus, it may be concluded that the cellulose/PVDF free-standing composite

films containing 42 wt% PVDF exhibit better hydrophobicity.

It is generally accepted that the modification of the surface properties and associated hydrophobic/hydrophilic characteristics could be related to the variation of surface energy arising from structural and bonding aspects of the material under study. The presence of numerous hydroxyl groups imparts strong polarity to cellulose. This is associated with strong inter- and intramolecular interactions, which account for its high crystallinity. In addition to the above, this renders cellulose poorly compatible with non-polar organic compounds, such as solvents and polymers. Several research attempts have been made to imitate nature in the formation of non-natural superhydrophobic surfaces. It was concluded that surface roughness and surface energy are the basic two key characteristics that would affect the hydrophobicity of a material. This would mean that knowledge of the morphological, structural and bonding environmental aspects of films with hydrophobic characteristics would be important. Such information could be of help to understand the observed hydrophobic behaviour of these cellulose/PVDF free-standing films.

It may be observed that the variation of contact angle with the PVDF content in the composite films did not vary linearly, as indicated in the inset of Figure 1 a. The remarked variation showed a similar trend to that observed for the variation of band gap for a ternary semiconductors.[21] This variation of contact angle could be fitted to a binomial expression as:

$$\theta(x) = A + Bx + Cx^2 \quad (1)$$

where $A = \theta_1$ and $\theta_2$ are the contact angles of PVDF ($x = 1$) and cellulose ($x = 0$), C is the bowing parameter, which could be evaluated from the data fit using the above expression (Eq. 1), by the least square fit method. It may be seen that the bowing parameter (C) was ~500°.

**FESEM studies**

The FESEM image of the pristine cellulose film (Fig. 2a) shows the presence of a ribbon-like filamentary structure. This filamentary structure would support external fibrillation for bonding improvement inside the basic fibrils. With the addition of PVDF to the cellulose, the morphology changed drastically, as evident from Figure 2 (b-d). One may observe that the surface consisted of numerous spherical bumps (Fig. 2d), which represented nanofibers. The presence of the above bumps decreased in the films when the PVDF content was increased beyond the critical value for which maximum hydrophobicity was observed. A nearly neat texture was observed for the pristine PVDF (Fig. 2e).

**XRD studies**

Figure 3 shows the XRD spectra of the pristine cellulose, pristine PVDF and cellulose/PVDF composite free-standing films, with three different PVDF loadings. It may be observed that the spectrum of the pristine cellulose film (inset of Fig. 3 a) indicated peaks located at $2\theta \sim 16.2^o$, $2\theta \sim 22.7^o$ and $2\theta \sim 34.8^o$. These peaks could be related to the characteristic peaks for the crystal form of cellulose-I polymorph. This result is in conformity with those reported by other authors.[22-23] The peak at $2\theta \sim 16.2°$ would correspond to the reflections from the (110) crystallographic plane for the non-crystalline component of cellulose. The peaks located at $2\theta \sim 22.7°$ and $2\theta \sim 34.8°$ would arise due to the reflections from the (002) for the crystalline component of cellulose and (023) or (004) planes, respectively.[24]

The XRD pattern obtained for the pristine PVDF film is shown in Figure 3 a. The peaks at $2\theta \sim 18.3^o$, $2\theta \sim 21.3^o$ and $2\theta \sim 22.4^o$ arising from the reflections from the (020), (110) and (111) planes could be identified as belonging to the α- and β-phase of PVDF, respectively. There are two other peaks at $2\theta \sim 26.6^o$ and $2\theta \sim 35.8^o$, arising from the reflections from the (021) and (002) planes of the PVDF α-phase. The peaks at $2\theta \sim 39.2^o$ and $2\theta \sim 43.0^o$ are attributed to the reflections from the (132) and (002) planes of the PVDF α-phase. The peaks at $2\theta \sim 47.4^o$, $2\theta \sim 48.4^o$ and $2\theta \sim 57.2^o$ arose due to the reflections from the (102), (122), (130) planes of PVDF, respectively.

The XRD spectra for the cellulose/PVDF composite free-standing films containing 33%, 42% and 70% PVDF are shown in Figure 3 b, c and d, respectively. All the spectra contain the signature peaks for both cellulose and PVDF located at $2\theta \sim 16.2°$, $2\theta \sim 22.7°$, $2\theta \sim 34.8°$ and $2\theta \sim 35.8°$. At this point, it can be noted that the peaks located at $2\theta \sim 16.2°$ arising from the non-crystalline component and the peak located at $2\theta \sim 22.7^o$ belonging to the crystalline component of cellulose are superposed with the peaks located at $2\theta \sim 18.3^o$ and $2\theta \sim 22.4^o$ attributed to the reflections from the (020) and (111) planes of

PVDF. The crystallinity of cellulose is generally evaluated from the diffraction intensity data of the peaks located at 2θ ~ 16.2° for the non-crystalline component and the peak located at 2θ ~ 22.7° for the crystalline component, using the empirical method for native cellulose.[25,26] Due to the superposition of the peaks indicated above, one has to be judicious enough to utilize the method for indicating any plausible change in the crystallinity of cellulose with the addition of PVDF. In the case of cellulose and PVDF as components in the resultant cellulose/PVDF composite free-standing films, the relative intensity values of the peaks located at 2θ ~ 16.2° and 2θ ~ 22.7° would vary more or less linearly (weighted mean value of the two constituents) with the addition of PVDF. A departure from the above would indicate possible modulation of the bonding environment of cellulose with the incorporation of PVDF. For this, we deconvoluted the above-mentioned peaks of the cellulose/PVDF composite films and estimated the relative intensities of the peaks located at 2θ ~ 16.2° and 2θ ~ 22.7° for the composite films. The variation of the relative intensities as a function of PVDF content in the composite films is shown in the inset of Figure 3 c. It may be observed that the variation of the relative intensity with the PVDF content showed a peak at ~42 wt%. This would mean that the crystallinity of cellulose increased significantly with the incorporation of PVDF. The crystallinity of cellulose then decreased with further addition of PVDF.

This information would suggest that the evolution of hydrophobicity in inherently hydrophilic cellulose is connected with the increased crystallinity of cellulose upon incorporation of PVDF. Other peaks located at 2θ ~ 39.2°, 2θ ~ 43.0°, 2θ ~ 47.4°, 2θ ~ 48.4° and 2θ ~ 57.3° are also visible, but with significantly lower intensities.

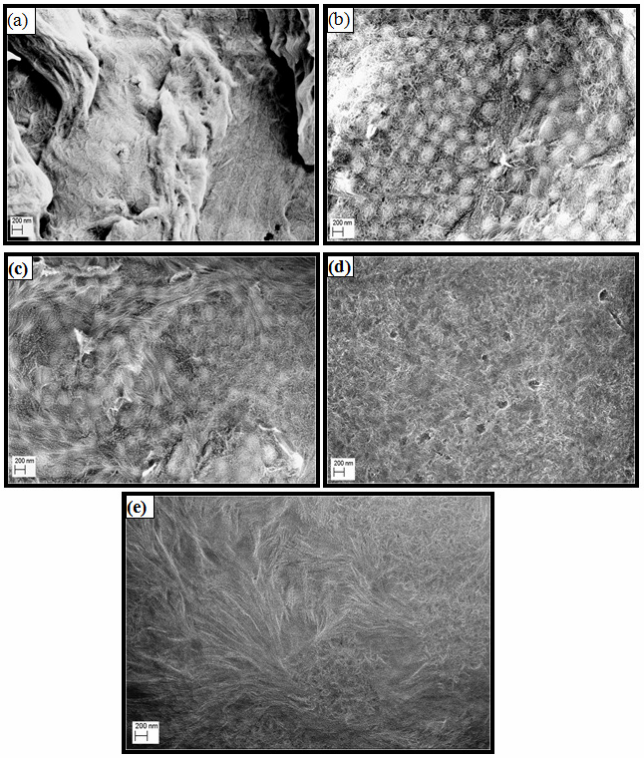


Figure 2: FESEM images of: (a) pristine cellulose film and cellulose/PVDF composite films with PVDF content of (b) 33%, (c) 42% and (d) 70%, and (e) pristine PVDF film

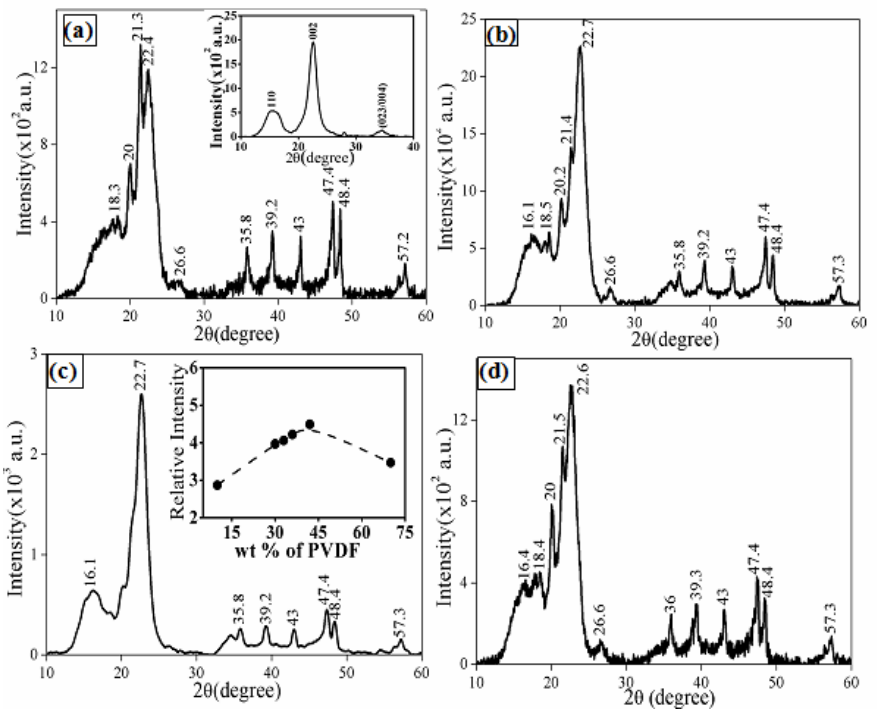


Figure 3: XRD patterns of: (a) pristine PVDF (inset shows the cellulose spectrum) and cellulose/PVDF composite films with (b) 33%, (c) 42% and (d) 70% PVDF content (inset in (c) shows the variation of relative intensity with PVDF concentration in cellulose/PVDF films

**FTIR studies**

The FTIR spectrum of the pristine PVDF sample is shown in Figure 4a. The peak at ~490 $cm^{-1}$ is due to the $CF_2$ vibrational modes of PVDF. The peak at 1070 $cm^{-1}$ is the characteristic peak related to the transverse optical (TO) mode. It originated from asymmetric stretching of the fluorine atoms along a direction parallel to the C-F direction for the β phase.[27] The band at 1400 $cm^{-1}$ could be ascribed to the $CH_2$ wagging mode of vibration. The band near 976 $cm^{-1}$ is due to the twisting mode of the $CH_2$ group. The strong bands located in the range ~845-873 $cm^{-1}$ could be ascribed to the $CH_2$ rocking modes. The band at ~1200 $cm^{-1}$ would represent coupling of $CF_2$ asymmetric stretching mode with C-C symmetric stretching mode. One may also observe a small peak at ~2358 $cm^{-1}$, along with the peak located at ~3024 $cm^{-1}$. It is known that the stretching modes of the $CH_2$ group generally appear in the frequency region from 2800 $cm^{-1}$ to 3000 $cm^{-1}$. The peaks appearing at ~2983 $cm^{-1}$ and 3024 $cm^{-1}$ would correspond to the symmetric and asymmetric modes of $CH_2$ vibrations. The FTIR spectrum for pristine cellulose fibers is shown in Figure 4b. The C–O–C stretching band at ~1022 $cm^{-1}$ appeared as skeletal vibration of cellulose. The stretching modes related to C-O, and C=C, and C-C-O of cellulose, hemicelluloses and lignin generally appear in the region of 1000-1058 $cm^{-1}$ in the FTIR spectra. The signature peak of the β-glycosidic linkages of cellulosic material is found at ~890 $cm^{-1}$ in all the samples.[24] The peak at ~1651 $cm^{-1}$ is due to $CF_2$ bending vibration. The 2900 $cm^{-1}$ peak could be assigned to the symmetric stretching modes of $CH_2$ group. The band at ~1651 $cm^{-1}$ could be ascribed to the C-O stretching mode of vibrations. The absorption bands located at ~3294 $cm^{-1}$ and 3402 $cm^{-1}$ would represent the C-H and O-H stretching vibrations, respectively.

Figure 4c shows the FTIR spectrum of a representative cellulose/PVDF free-standing composite film containing 42% PVDF. A modulation of the FTIR spectrum of cellulose (Fig. 4b) with the addition of PVDF is apparent from it. The signature peaks for PVDF and cellulose appearing in the range of 490-1400 $cm^{-1}$ are suppressed significantly. Some lower intensity peaks located at ~550 $cm^{-1}$, ~675 $cm^{-1}$, 775 $cm^{-1}$,

1253 $cm^{-1}$, 1382 $cm^{-1}$, 2854 $cm^{-1}$, 3272 $cm^{-1}$ and 3560 $cm^{-1}$ could be observed. Most of the FTIR peaks related to pristine cellulose fibers and PVDF are absent in these composite films.[28,29] The above observation is true for all the cellulose/PVDF composite films studied here. The low intensity peak located at ~675 $cm^{-1}$ could be ascribed to the COOH out-of-plane bonding vibrations. The peaks around 3272 $cm^{-1}$ and 3560 $cm^{-1}$ could be associated to the formation of a new hydroxyl group –OH bonding with the interaction with PVDF. The peak located at ~2357 $cm^{-1}$ could be due to the appearance of additional -C-H- and –C-F- bonding with the addition of PVDF in cellulose. The changed bonding environment may offer a repelling force to the polar water molecules, favouring the hydrophobic characteristics of the composite cellulose/PVDF free-standing films. The peaks at ~3272 $cm^{-1}$ would bear the signature of O-H stretching from intra- and intermolecular hydrogen bonding associated with cellulose with the addition of PVDF. The FTIR absorption band at ~1452 $cm^{-1}$ is generally assigned to symmetric $CH_2$ bending vibration. This band is also referred to as the "crystallinity band". The FTIR absorption band at 893 $cm^{-1}$ may be assigned to C–O–C stretching at β-(1→4)-glycosidic linkages, which may be designed as an "amorphous" absorption band.

**Raman studies**

Raman spectra of pristine cellulose and PVDF are shown in Figure 5 a and b, respectively. The Raman spectra of pristine cellulose fibers exhibit a strong peak at ~378 $cm^{-1}$, followed by peaks appearing at ~170 $cm^{-1}$, 330 $cm^{-1}$, 436 $cm^{-1}$, 507 $cm^{-1}$, 564 $cm^{-1}$, 899 $cm^{-1}$ and 968 $cm^{-1}$. The bending modes of COC, CCC, OCC and OCO are mainly dominant in the region of 150 $cm^{-1}$-550 $cm^{-1}$. The peak at ~170 $cm^{-1}$ represents the COH methane bending mode. The peak at ~378 $cm^{-1}$ is attributed to the characteristic mode of amorphous cellulose and is present in all the films.[30,31] A peak of relatively weaker intensity is observed at ~436 $cm^{-1}$, which can be assigned to OCC bending. The peaks appearing in the range of ~850 $cm^{-1}$-1000 $cm^{-1}$ are due to the presence of C-O and C-C stretching modes, as well as to the HCC and HCO bending modes. The peaks at ~899 $cm^{-1}$ and ~904 $cm^{-1}$ are due to the presence of HCC, HCO bending modes only. The peak appearing at ~968 $cm^{-1}$ could be assigned to HCH bending modes.

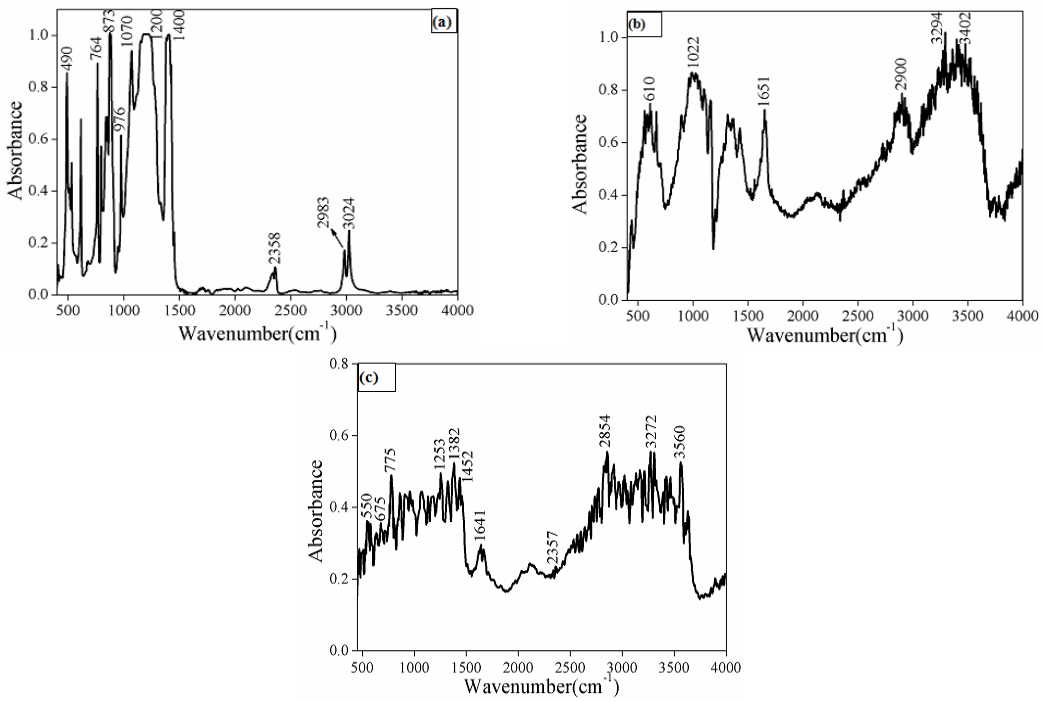


Figure 4: FTIR spectra of four representative films: (a) pristine PVDF, (b) pristine cellulose and (c) cellulose/PVDF composite film with PVDF content of ~42%

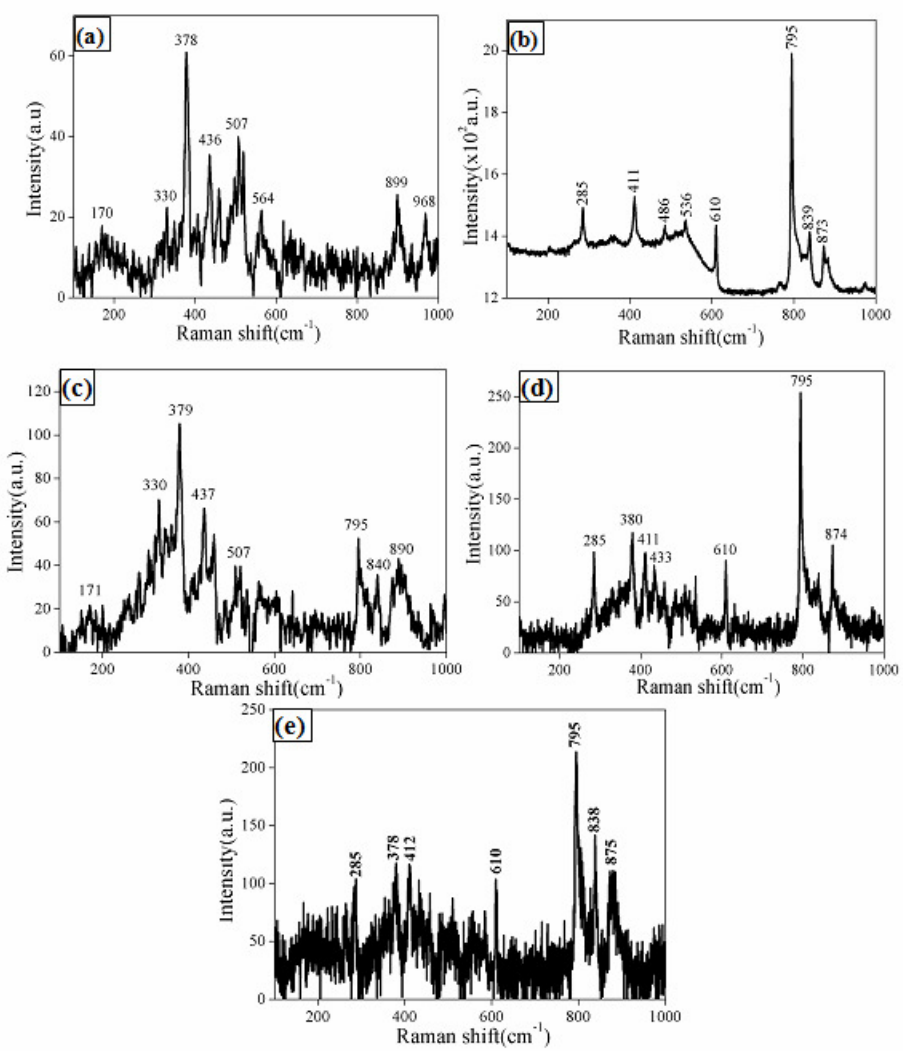


Figure 5: Raman spectra for four representative films: (a) pristine cellulose, (b) pristine PVDF and cellulose/PVDF composite films with different PVDF content: (c) 33%, (d) 42% and (e) 70%

The intensity of the characteristic peaks of pristine PVDF appearing in the spectra (Fig. 5b) was nearly similar for all the PVDF films synthesized in this study. The Raman spectrum of the PVDF film contained peaks located at ~285 $cm^{-1}$, ~411 $cm^{-1}$, ~536 $cm^{-1}$, ~610 $cm^{-1}$, ~795 $cm^{-1}$, ~839 $cm^{-1}$ and ~873 $cm^{-1}$ (Fig. 5b). The TG sequence for PVDF appeared at ~795 $cm^{-1}$. This observation supports the results Boccaccio *et al.*[32] The weak band located at ~839 $cm^{-1}$ could be assigned to T3G sequences in the PVDF matrix. The presence of either γ, β or both phases in the PVDF film is indicated by the peak appearing at ~839 $cm^{-1}$, while the presence of both α- and β-phases is indicated by the presence of the peak located at ~1132 $cm^{-1}$ (Fig. 5b).

Additionally, the band at ~839 $cm^{-1}$ may also appear due to the presence of out-of-phase $CH_2$ rocking modes. A shift in the characteristic peaks of the pristine cellulose (Fig. 5a) and PVDF (Fig. 5b) is apparent in the Raman spectra of the three representative cellulose/PVDF composite free-standing films, with increasing PVDF content in the film (Fig. 5c-e). The strong band appearing at ~795 $cm^{-1}$ for the PVDF film has shifted significantly in the spectrum of the composite film (Fig. 5c-e). The relative intensities of the peak at ~378 $cm^{-1}$ representing the characteristic mode for amorphous cellulose and that at ~795 $cm^{-1}$ for PVDF decreased significantly with increasing PVDF content from 33% (Fig. 5c) to ~42% (Fig. 5d). With further increase in the

PVDF content, they increased again for the composite film with 70% PVDF content (Fig. 5e). This would mean that the amorphous cellulose content decreased with the addition of up to 42% PVDF to the cellulose, and thus the crystallinity of cellulose increased. With further addition of PVDF, the crystallinity of cellulose decreased in the composite films. It may be noted here that the films with higher PVDF content (>42 wt%) tended to show inferior hydrophobic characteristics. Thus, increased cellulose crystallinity in the composite films would render higher hydrophobicity.

**Possible explanation of hydrophobicity in free-standing cellulose/PVDF composite films**

Cellulose is a linear polysaccharide, composed of repeating β-1,4-D-glucose units, with a typical polymerization degree in the range from 10,000 to 15,000 depending on the source.[33] It is known that strong inter- and intramolecular interactions originated from the hydroxyl groups are present in cellulose. These, in turn, would govern the physical properties of cellulose, including its inherent hydrophilic characteristic. This would mean that it would be possible to change the hydrophilic character of cellulose through surface modification using hydrophobic compounds.[4-7] Recently, researchers have focused on the surface hydrophobization of cellulose by the use of physical and chemical modification methods.[34-38] Structural anisotropy is the basis of the hydrophilic/hydrophobic nature of cellulose. It has been reported that increased crystallinity in microcrystalline cellulose facilitates hydrophobicity in cellulose.[7] Our XRD results are in conformity with these findings.

Understanding hydrophobicity on different surfaces, Wenzel put forward a relationship for the dependence of contact angles on the roughness parameter (r) defined by the ratio of the real surface area to the projected surface area.[39] He suggested that for $r >> 1$, a surface would be hydrophobic with $\theta > 90^o$. For a hydrophilic surface with $\theta < 90^o$, roughness has the opposite effect ($r<<1$). Although the Wenzel equation is valid when the liquid droplet enters the valleys and completely wets the surface topography, the Cassie–Baxter model requires the presence of a liquid–vapor interface below the droplet.[40] It was suggested that at constant surface roughness, the surface chemistry can be designed to have the contact angle behavior to go from the Wenzel regime to the Cassie–Baxter regime. It must be noted here that the above theories are valid for surfaces of simple materials, but not for composite materials. Thus, with regard to the cellulose/PVDF free-standing films developed in this study, the observed variation of contact angle may not be described faithfully by these theories.

In the case of pristine cellulose, the water molecules will bond easily with molecules with an opposite charge that approach them. Two hydrogen atoms bonded to an oxygen atom would constitute a water molecule. Two pairs of unshared electrons would also be carried by them, additionally forming bonds with the hydrogen atoms. This makes the pristine cellulose inherently hydrophilic. When PVDF is added to cellulose, the PVDF with its hydrogen and fluorine terminated surface would modulate the intra-chain and inter-chain hydrogen bonding environment in cellulose. This would result in additional -C-H- and –C-F- bonding at the surface, which would facilitate the formation of a hydrophobic surface. The presence of a primary OH group at the C6 position would perturb the symmetry.[5] An attractive force will be experienced by a hydrogen atom attached to the electronegative atom of a molecule (here water) and the electronegative atom of a different molecule (fluorine of PVDF). The electronegative atom in question is generally oxygen, nitrogen, or fluorine, having a partial negative charge. As flourine is more electronegative than hydrogen, the F atom would hog electrons and keep them away from the H atoms. This would make the oxygen end of the water molecule experience a partial negative charge, while the hydrogen end would experience a partial positive charge. This would facilitate repulsion of water from the cellulose/PVDF composite surface. The FTIR and Raman spectroscopic analyses carried out in the present study also supported such modification of the bonding environment.

**CONCLUSION**

It may be concluded from this work that hydrophobic characteristics can be imparted to cellulose fibers by the addition of PVDF, to produce free-standing cellulose/PVSD composite films. The modulation of the intra- and interchain hydrogen bonding in cellulose with the addition of PVDF resulted in the formation of additional -C-H- and –C-F- bonding on the surface, which facilitated the development of a hydrophobic surface. The associated increase in the crystalline components in cellulose represented an additional

advantage, facilitating the hydrophobic characteristics of cellulose. The hydrophobicity of the prepared films was studied by examining the contact angle of the water droplets placed on them. The contact angle increased from $10^o$ to $147^o$ with the increase in the PVDF content in the film and then decreased with further addition of PVDF. The highest contact angle ($147^o$) was obtained for the cellulose/PVDF composite films with 42 wt% PVDF, which thus exhibited the highest hydrophobicity.

***ACKNOWLEDGEMENTS***: R. Dey wishes to acknowledge with thanks financial help through the DST-INSPIRE fellowship programme of the Department of Science and Technology, Government of India. Thanks are also due to Manoj Adak and Ratnadeep Roy, both M.Sc. students of our department, for their assistance in casting cellulose films and recording the water droplet images, respectively.

## REFERENCES

[1] S. M. Arteta, R. Vera and L. D. Pérez, *J. Appl. Polym. Sci.*, **134**, 44482 (2016), https://doi.org/10.1002/app.44482

[2] S. Tanpichaia, S. Witayakran, Y. Srimarut, W. Woraprayote and Y. Malila, *J. Mater. Res. Technol.*, **8**, 3612 (2019), https://doi.org/10.1016/j.jmrt.2019.05.024

[3] H. Águas, T. Mateus, A. Vicente, D. Gaspar, M. J. Mendes *et al.*, *Adv. Funct. Mater.*, **25**, 3592 (2015), https://doi.org/10.1002/adfm.201500636

[4] T. A. Dankovich and Y. Lo Hsieh, *Cellulose*, **14**, 469 (2007), https://doi.org/10.1007/s10570-007-9132-1

[5] J. K. Dutkiewicz, S. A. Skirius, S. M. Fields, L. H. Rushing, D. J. Smith *et al.*, US Patents US8946100B2 (2006), https://patents.google.com/patent/US8946100B2/en

[6] X. Huang, A. Wang, X. Xu, H. Liu and S. Shang, *ACS Sustain. Chem. Eng.*, **5**, 1619 (2017), https://doi.org/10.1021/acssuschemeng.6b02359.

[7] K. Awa, H. Shinzawa and Y. Ozaki, *AAPS Pharm. Sci. Tech.*, **16**, 865 (2015), https://doi.org/10.1208/s12249-014-0276-7

[8] C. Yu, F. Wang, L. A. Lucia and S. Fu, *Adv. Mater. Phys. Chem.*, **7**, 395 (2017), https://doi.org/10.4236/ampc.2017.712031

[9] M. He, M. Xu and L. Zhang, *ACS Appl. Mater. Interfaces*, **5**, 585 (2013), https://doi.org/10.1021/am3026536

[10] A. Adewuyi and F. V. Pereira, *J. Sci. Adv. Mater. Dev.*, **2**, 326 (2017), https://doi.org/10.1016/j.jsamd.2017.07.007

[11] Y. Wang, L. Liu, P. Chen, L. Zhang and A. Lu, *Phys. Chem. Chem. Phys.*, **20**, 14223 (2018), https://doi.org/10.1039/c8cp01268g

[12] T. Huang, C. Chen, D. Li and M. Ek, *Cellulose*, **26** 665 (2019), https://doi.org/10.1007/s10570-019-02265-8

[13] F. Mikaeili and P. I. Gouma, *Sci. Rep.*, **8**, 12472 (2018), https://doi.org/10.1038/s41598-018-30693-2

[14] Z. Yuan and Y. Wen, *Cellulose*, **25**, 6863 (2018), https://doi.org/10.1007/s10570-018-2048-0

[15] J. Lim and J. R. Kim, *Cellulose*, https://doi.org/10.1007/s10570-019-02959-z

[16] S. Sakurai, Y. Akiyama and H. Kawasaki, *R. Soc. Open Sci.*, **5**, 172417 (2018), https://doi.org/10.1098/rsos.172417

[17] J. Perelaer, P. J. Smith, D. Mager, D. Soltman, S. K. Volkman *et al.*, *J. Mater. Chem. C*, **20**, 8446 (2010), https://doi.org/10.1039/C0JM00264J

[18] Y. Zhan, Y. Mei and L. Zheng, *J. Mater. Chem. C*, **2**, 1220 (2014), https://doi.org/10.1039/C3TC31765J

[19] T. Yang, D. Xie, Z. Li and H. Zhu, *Mater. Sci. Eng. R*, **115**, 1 (2017), https://doi.org/10.1016/j.mser.2017.02.001

[20] S. Liang, Y. Kang, A. Tiraferri, P. Giannelis, X. Huang *et al.*, *ACS Appl. Mater. Interfaces*, **5**, 6694 (2013), https://doi.org/10.1021/am401462e

[21] R. Hill, *J. Phys. C: Solid State Phys.*, **7**, 521 (1974), https://doi.org/10.1088/0022-3719/7/3/009

[22] L. A. D. S. Costa, A. F. Fonseca, F. V. Pereira and J. I. Druzian, *Cellulose Chem. Technol.*, **49**, 127 (2015), https://www.cellulosechemtechnol.ro/pdf/CCT2(2015)/p.127-133.pdf

[23] M. M. De Souza Lima and R. Borsali, *Macromol. Rapid Commun.*, **25**, 771 (2004), https://doi.org/10.1002/marc.200300268

[24] M. P. Adinugraha, D. W. Marseno and Haryadi, *Carbohyd. Polym.*, **62**, 164 (2005), https://doi.org/10.1016/j.carbpol.2005.07.019

[25] S. M. Rosa, N. Rehman, M. I. G. de Miranda, S. M. B. Nachtigall and C. I. D. Bica, *Carbohyd. Polym.*, **87**, 1131 (2012), https://doi.org/10.1016/j.carbpol.2011.08.084

[26] M. Schwanninger, J. C. Rodrigues, H. Pereira and B. Hinterstoisser, *Vib. Spectrosc.*, **36**, 23 (2004), https://doi.org/10.1016/j.vibspec.2004.02.003

[27] L. N. Sim, S. R. Majid and A. K. Arof, *Vib. Spectrosc.*, **58**, 57 (2012), https://doi.org/10.1016/j.vibspec.2011.11.005

[28] D. Das, S. Hussain, A. K. Ghosh and A. K. Pal, *Cellulose Chem. Technol.*, **52**, 729 (2018), https://www.cellulosechemtechnol.ro/pdf/CCT9-10(2018)/p.729-739.pdf

[29] R. Dey, R. Bhunia, S. Hussain, B. R. Chakraborty, R. Bhar *et al.*, *Polym. Plast. Technol. Eng.*, **56**, 310

(2017), https://doi.org/10.1080/03602559.2016.1233252
[30] K. Schenzel and S. Fischer, *Lenzinger Berichte*, **83**, 64 (2004), https://pdfs.semanticscholar.org/5cd5/648c6f5839be5f89fbc1e910a32e1cdb3870.pdf
[31] L.-L. Cho, *Forensic Sci. J.*, **6**, 55 (2007), http://lawdata.com.tw/tw/detail. aspx? no=182253
[32] T. Boccaccio, A. Bottino, G. Capannelli and P. Piaggio, *J. Memb. Sci.*, **210**, 315 (2002), https://doi.org/10.1016/S0376-7388(02)00407-6
[33] R. J. Moon, A. Martini, J. Nairn, J. Simonsen and J. Youngblood, *Chem. Soc. Rev.*, **40**, 3941 (2011), https://doi.org/10.1039/C0CS00108B
[34] S. Mondal, *Carbohyd. Polym.*, **163**, 301 (2017), https://doi.org/10.1016/j.carbpol.2016.12.050
[35] J. C. Natterodt, J. Sapkota, E. J. Foster and C. Weder, *Biomacromolecules*, **18**, 517 (2017), https://doi.org/10.1021/acs.biomac.6b01639
[36] X. Niu, Y. T. Liu, Y. Song, J. Q. Han and H. Pan, *Carbohyd. Polym.*, **183**, 102 (2018), https://doi.org/10.1016/j.carbpol.2017.11.079
[37] M. Peng, H. Li, L. Wu, Q. Zheng, Y. Chen *et al.*, *J. Appl. Polym. Sci.*, **98**, 1358 (2005), https://doi.org/10.1002/app.22303
[38] Q. Shang, C. Liu, Y. Hu, P. Jia, L. Hu *et al.*, *Carbohyd. Polym.*, **191**, 168 (2018), https://doi.org/10.1016/j.carbpol.2018.03.012
[39] R. N. Wenzel, *Ind. Eng. Chem.*, **28**, 988 (1936), https://pubs.acs.org/ doi/pdf/ 10.1021/ie50320a024
[40] A. B. D. Cassie and S. Baxter, *Trans. Faraday Soc.*, **40**, 546 (1944), https://pubs.rsc.org/en/content/articlepdf/1944/tf/tf9444000546